IEEJ Journal of Industry Applications
Vol.6 No.5 pp.303–310 DOI: 10.1541/ieejjia.6.303

Paper

Voltage Rise Suppression and Load Balancing by PV-PCS with Constant DC-Capacitor Voltage-Control-Based Strategy in Single-Phase Three-Wire Distribution Feeders

Mitsumasa Ushiroda* Non-member, Takaaki Wakimoto* Non-member
Hiroaki Yamada* Member, Toshihiko Tanaka*a) Fellow
Masayuki Okamoto** Member, Koji Kawahara*** Senior Member

(Manuscript received Sep. 9, 2016, revised May 23, 2017)

This paper proposes a voltage-rise-suppression strategy with a power quality compensator for a roof-top home solar power system (HSPS) connected to the point of common coupling (PCC) in single-phase three-wire distribution feeders (SPTWDFs). The proposed reactive power control and power quality compensation strategy uses only a constant dc-capacitor voltage control, which is always used in grid-connected inverters. No calculation blocks of the reactive and unbalanced active components of the load currents are necessary. Thus, the authors provide the simplest algorithm to suppress the voltage rise at the PCC with power quality compensation. The basic principle of the constant dc-capacitor voltage-control-based strategy is discussed in detail. The instantaneous power flowing into the HSPSs shows that the predefined power factor of 0.9, a value that conforms to the Japanese regulations, is achieved with improved-quality source-currents of domestic consumers connected to SPTWDFs, suppressing the voltage rise at the PCC. A digital computer simulation is implemented to confirm the validity and high practicability of the proposed control algorithm for HSPSs using a typical SPTWDF model in Japan. Simulation results demonstrate that the proposed control method for the roof-top HSPS suppresses the voltage rise at the PCC, improving the source-side power quality.

Keywords: photovoltaic power generation system, voltage-rise-suppression, constant dc-capacitor voltage control, reactive power control, power quality compensator, single-phase three-wire distribution feeder

1. Introduction

Renewable energy has attracted a great deal of attention after the Great East-Japan Earthquake of 2011. The Act on Special Measures Concerning Procurement of Electricity from renewable energy sources by electricity utilities was enacted on August 30, 2011 [(1)]. According to this act, Japanese domestic electricity utilities are obligated to purchase power generated by solar, wind, hydro, geothermal, and biomass plants. The procurement price and period are decided annually by the Minister of Economy, Trade and Industry (METI). After the enactment of the act, a large number of photovoltaic power generation systems (PVPGSs) have been constructed. Japanese domestic electricity utilities are also obligated to purchase power generated by home solar power systems (HSPSs), where the rating of PV cells is less than 10 kW. The HSPSs can sell the surplus of the generated power and the power consumed at home. A large number of houses have been equipped with rooftop PVs in Japan. Voltage-source pulse-width modulated (PWM) inverters are used as an interface between PVs and utility-grids. The generated power is injected to the utility-grids with unity power factor by voltage-source PWM inverters. In general distribution systems are designed with unidirectional power flows, supplying power from power plants to consumers. It is well known that reverse power flows with unity power factor by voltage-source PWM inverters in highly spreaded PVPGSs cause an unacceptable voltage rise at the point of common coupling (PCC) [(2)].

Active power curtailment has been proposed for voltage-rise mitigation [(3)]. However, active power curtailment is not an economical solution for a domestic consumer. Economic output power losses caused by the voltage rise at the PCC have been reported [(4)(5)]. A reactive power consumption for voltage-rise suppression also has been proposed [(6)–(8)]. The reactive power consumption may create additional loss in feeders caused by a larger current flow [(9)]. An alternative solution is a combination of a HSPS and an energy storage system (ESS) [(10)–(13)]. The HSPSs with the ESS are effective to mitigate the voltage-rise problems in low-voltage feeders. The HSPSs with the ESS also contribute to level the power from the utility-grid, which is consumed by domestic consumers. A battery in electric vehicles (EVs) is used as an ESS in (14). EVs are highly mobile with the stored electric power. As a

a) Correspondence to: Toshihiko Tanaka. E-mail: totanaka@yamaguchi-u.ac.jp
* Department of Electrical and Electronic Engineering, Yamaguchi University
2-16-1, Tokiwadai, Ube, Yamaguchi 755-8611, Japan
** Department of Electrical Engineering, National Institute of Technology, Ube College
2-14-1, Tokiwadai, Ube, Yamaguchi 755-8555, Japan
*** Department of Electrical Systems Engineering, Hiroshima Institute of Technology
2-1-1, Miyake, Saeki-ku, Hiroshima 731-5193, Japan

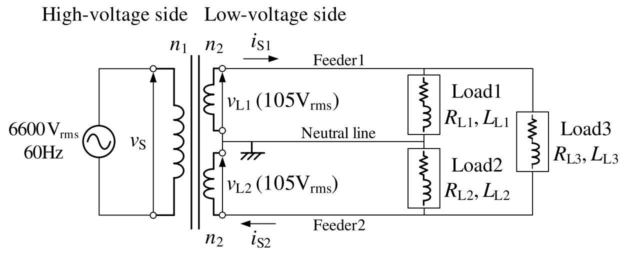

Fig. 1. Typical single-phase three-wire distribution feeder (SPTWDF) in Japan

result of this mobility, the interesting concept to inject the stored power of EVs into grid, and home (Vehicle-to-Grid, and Vehicle-to-Home) has been proposed [15]–[18]. Thus, the advantage of this highly mobile with the stored electric power has not been discussed. According to (1), the price of the power generated by roof-top HSPSs, which is purchased by power companies, is higher than that of the power supplied to domestic consumers from power companies. This means that storing the power generated by roof-top HSPSs in the ESSs reduces the profit by the sale of the power generated roof-top HSPSs. Thus, selling all surplus power between the power generated by a roof-top HSPS and the power consumed by a domestic consumer is economically effective in Japan.

SPTWDFs are used for domestic consumers in Japan. Figure 1 shows a typical SPTWDF. Home appliances in Japan are divided into two types depended on their capacity. Large-capacity loads are connected to Feeder1 and Feeder2, and their voltage rating is 210 Vrms. These large-capacity home appliances, which include air conditioners and IH cookers, are equipped with PFC rectifiers and inverters. Other small-capacity loads are connected to each feeder with a neutral line, and their voltage rating is 105 Vrms. The voltage at the PCC in these SPTWDFs should be less than 107 Vrms, according to Japanese regulations [19]. If the voltage at the PCC exceeds 107 Vrms, power companies have to restrict the output power of the HSPS. This restriction occurs at midday with fine weather. As described above, this is a serious problem for HSPSs because the profit from the sale of power decreases. A reactive power consumption for voltage-rise suppression is effective. However, the reactive power consumption method proposed in (6)–(8) cannot be applied to Japanese SPTWDFs. The overvoltage correction with reactive power control has been discussed in detail for roof-top HSPSs of domestic consumers [20]. Three-phase grids are used in Greece for domestic consumers. Thus, the proposed overvoltage correction strategy also cannot be applied to Japanese SPTWDFs. In Fig. 1, the source-side currents i_{S1} and i_{S2} are always unbalanced due to the unbalanced load conditions. These unbalanced source currents conditions cause the unbalanced terminal voltages v_{L1} and v_{L2}. It is well known that these unbalanced source current conditions increase the losses in the pole-mounted distribution transformers (PMDTs). Thus, not only voltage-rise-suppression with reactive power control but also power quality compensation, which is to balance the secondary-side currents of the PMDTs, are required for roof-top HSPSs in SPTWDFs in Japan.

This paper proposes a voltage-rise-suppression and power quality compensation strategy for the HSPSs connected to the PCC in SPTWDFs. For a control strategy of roof-top HSPSs, a constant dc-capacitor voltage-control-based reactive power control algorithm is used. The constant dc-capacitor voltage-control-based control strategy [21] can suppress the voltage rise caused by roof-top HSPSs improving power quality on the secondary-side currents of the PMDTs. The proposed reactive power control with power quality compensator uses only a constant dc-capacitor voltage control, which is always used in the grid-connected inverters. Any calculation blocks of the reactive and unbalanced active components of the load currents are not necessary. Thus, the authors provide the simplest algorithm to suppress the voltage rise at the PCC with the balanced source-side currents. Improving the source-side currents quality reduces the losses in the PMDTs. This means that the created-additional loss in feeders caused by a larger current flow caused by the reactive power consumption can be mitigated [9]. The basic principle of the constant dc-capacitor voltage-control-based strategy is discussed in detail. The instantaneous power flowing into the power conditioning system (PCS) of HSPS shows that the predefined power factor of 0.9, which is a value that conforms to Japanese regulations [22], is achieved with the balanced source currents for domestic consumers connected to SPTWDFs with the constant dc-capacitor voltage-control-based strategy, suppressing the voltage rise at the PCC. A digital computer simulation is implemented to confirm the validity and high practicability of the proposed control algorithm for the HSPS using a typical SPTWDF in Japan. The simulation results demonstrate that controlling the power factor to 0.9 on the source side by the HSPS with the proposed control method suppresses the voltage rise at the PCC, improving the source-side currents quality.

2. Proposed Voltage-rise-suppression and Power Quality Compensation with Reactive Power Control for HSPSs

2.1 Low-voltage Distribution Feeder Model

SPTWDFs are used in residential areas of Japan. Figure 2 shows a typical SPTWDF in a residential area [23]. A PMDT is used to deliver power to domestic consumers. The rating of the PMDT is 6.6 kVrms, 45 kVA, and 60 Hz on the primary side and 105 Vrms and 214 Arms on the secondary side. Three low-voltage wires of 30 m with three nodes are connected on the secondary side of the PMDT. Power is supplied to three domestic consumers, which have the same load conditions at Node1, Node2, and Node3, respectively. The domestic consumer receives power through a 15 m service-wire. Another domestic consumer receives power through a 20 m service-wire. Yet another domestic consumer receives power through a 25 m service-wire. At Node3, three domestic consumers have HSPSs, where the rating of an HSPS is 4.0 kW. Thus, nine domestic consumers connected to the distribution feeder of Fig. 2 are considered. Table 1 shows the impedances for low voltage and service wires. Table 2 shows the circuit constants for Fig. 2. The circuit constants of Table 2 were determined on the basis of the constants of Table 1 and the lengths of wires. In the typical residential areas of Japan, two-income families are the norm. In these two-income families, nobody resides in their houses during

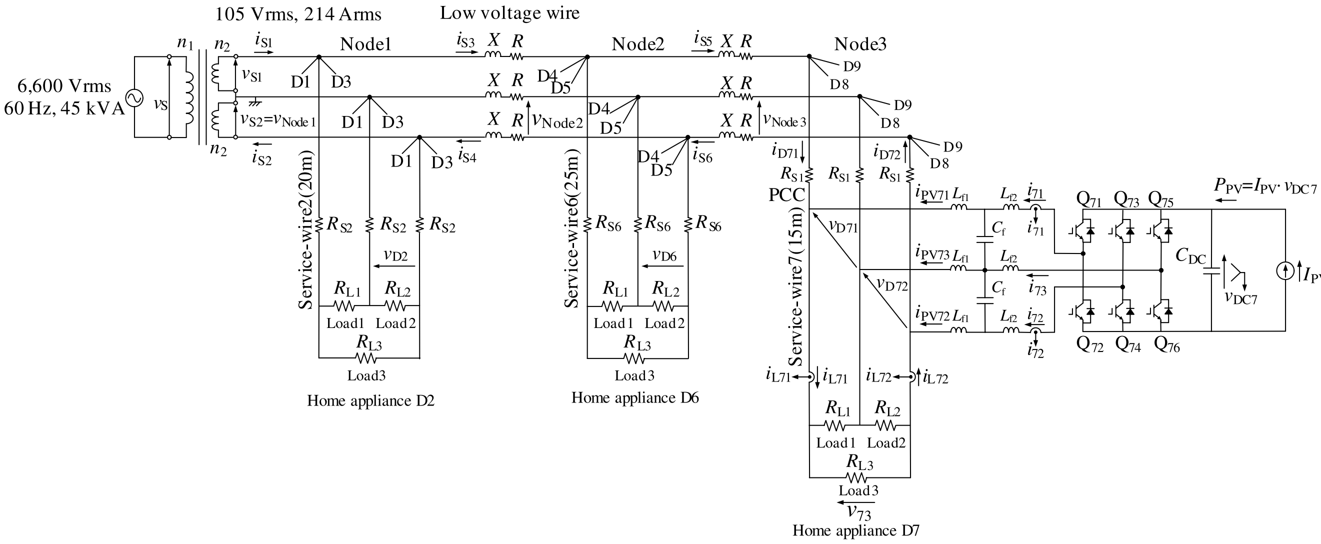

Fig. 2. Power circuit diagram of typical SPTWDF model with HSPSs

Table 1. Impedances for low-voltage and service wires

Item	Resistance	Reactance
Low voltage wire	0.484 Ω/km	0.343 Ω/km
Service wire	2.58 Ω/km	

Table 2. Circuit Constants for Fig. 2

Item	Symbol	Value
Low Voltage wire Impedance(30 m)	R	14.5 mΩ
	X	10.3 mΩ
Service wire Impedance(20 m)	R_{S2}	51.6 mΩ
Service wire Impedance(25 m)	R_{S6}	64.5 mΩ
Service wire Impedance(15 m)	R_{S7}	38.7 mΩ
Load1 (300 W)	R_{L1}	36.8 Ω
Load2 (200 W)	R_{L2}	55.1 Ω
Load3 (100 W)	R_{L3}	441 Ω
Filter inductor	L_{f1}	0.5 mH
	L_{f2}	1.0 mH
Filter capacitor	C_f	10.4 μF
dc capacitor	C_{DC}	3000 μF
dc-capacitor voltage	V_{DC}	385 Vdc
PV-current (4.0 kW)	I_{PV}	10.4 Adc
Switching frequency	f_{SW}	12 kHz

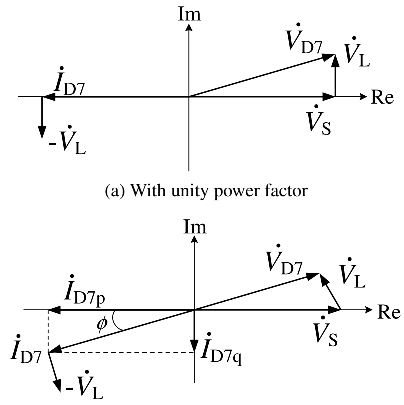

(a) With unity power factor

(b) With reactive power control

Fig. 3. Phasor diagrams at the PCC on Service-wire7

the daytime. Only standby power consumption exists in all domestic consumers. Typical standby power consumption is 5.1% as compared to the total power consumption in a domestic consumer [24]. Considering this standby power consumption with a power consumption caused by a few consumer electronics, the load conditions of R_{L1}, R_{L2}, and R_{L3} were decided in (23). On the other hand, the correct load conditions for all domestic consumers in Fig. 2 cannot be decided. The load conditions for all domestic consumers are identical in (23). Thus, for all domestic consumers, an R_{L1} of 36.8 Ω is connected to the 105 Vrms upper-side feeder, an R_{L2} of 55.1 Ω is connected to the 105 Vrms lower-side feeder, and an R_{L3} of 441 Ω is connected to the 210 Vrms feeder, where total consumption power is 600 W, which is 12% in a domestic consumer.

In the literature (23), the voltage-rise phenomenon at Node3, which is caused by the roof-top HSPSs, has been demonstrated. Fig. 3 shows the phasor diagrams at the PCC on Service-wire7. $\dot{I}_{D7}$ corresponds to the output currents i_{D71} and i_{D72}. $\dot{V}_{D7}$ is for the terminal voltages v_{D71} and v_{D72} at the PCC on Service-wire7. $\dot{V}_S$ is for the secondary-side voltages v_{S1} and v_{S2} of the PMDT. In Fig. 3(a), the output current $\dot{I}_{D7}$ of the roof-top HSPS is injected with unity power factor. $\dot{V}_L$ is caused by the line inductor on the low-voltage wires and the service wires. The terminal voltage $\dot{V}_{D7}$ is given by the sum of $\dot{V}_S$ and $\dot{V}_L$. Thus, the amplitude of $\dot{V}_{D7}$ is larger than that of $\dot{V}_S$. This is the voltage-rise phenomenon caused by the HSPS, which is a serious problem, because the profit from the sale of power decreases. In Fig. 3(b), the output current $\dot{I}_{D7}$ of the HSPS is injected with reactive power control. The phase angle ϕ can be controlled with the reactive component I_{D7q}. The amplitude of $\dot{V}_{D7}$ can be controlled with $\dot{I}_{D7q}$. Controlling $\dot{I}_{D7q}$ can avoid the voltage rise of $\dot{V}_{D7}$ at the PCC.

2.2 Voltage-rise-suppression and Power Quality Compensation with Reactive Power Control Figure 4 shows a power circuit diagram and the control block diagram for the HSPS on Service-wire7 with the constant dc-capacitor voltage-control-based reactive power control. Note that only the part enclosed by the dotted line is added to the constant dc-capacitor voltage control, which is always used in the grid-connected inverter, to control the reactive power on the source side.

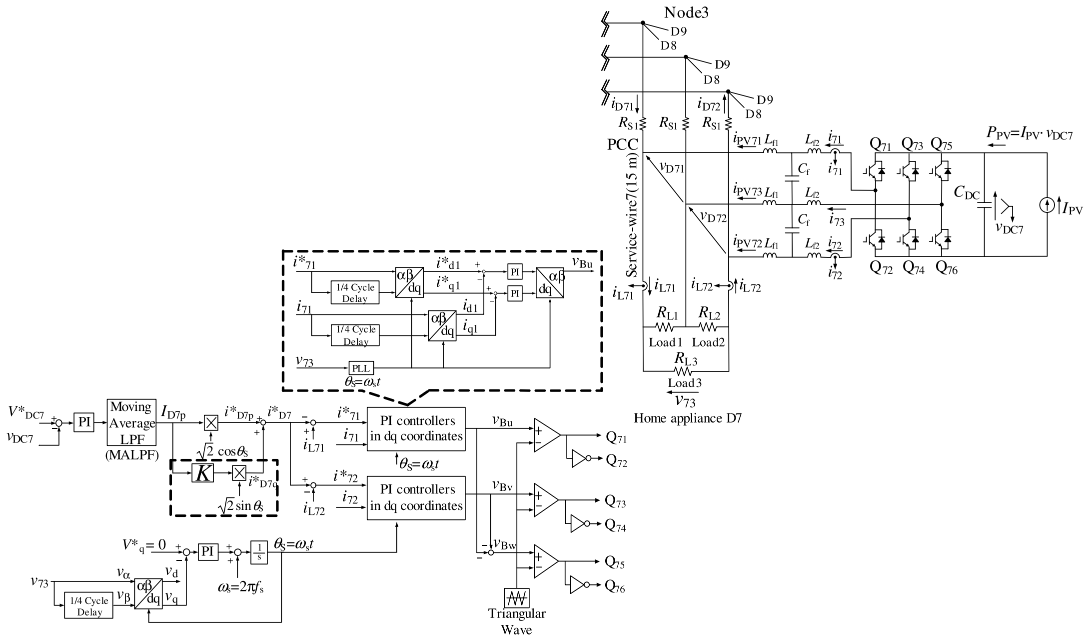

Fig. 4. Power circuit diagram and control block diagram for HSPSs on Service-wire7 with constant dc-capacitor voltage-control-based reactive power control

In three-phase circuits, some control strategies in these active power line conditioners are based on active-reactive instantaneous power theory, which was originally proposed by Prof. H. Akagi [25]–[29]. The instantaneous symmetrical component theory method, the sample and hold circuit method and *d*-*q* transformation based method are also used for the calculation of the reference compensation currents [30]–[32]. The present authors also proposed a control method to reduce the capacity of the three-leg PWM rectifier, which performs a smart charger for electric vehicles in SPTWDFs [33]. However, in the proposed control method, the calculation blocks of the load-side active and reactive currents in addition to the constant dc- capacitor voltage control block are needed to achieve a source-side power factor of 0.9. In Fig. 4, however, no calculation blocks of the reactive and unbalanced active components of the load currents are necessary.

On the other hand, no calculation blocks of the reactive and unbalanced active components of the load currents are necessary in Fig. 4. Thus, the authors provide the simplest algorithm to suppress the voltage rise at the PCC with balanced source-side currents. The basic principle of the constant dc-capacitor voltage-control-based algorithm is discussed. The voltages v_{D71} and v_{D72} on D7, and the load currents i_{L71} and i_{L72} in Fig. 4 are given as

$$\begin{aligned} v_{D71} &= v_{D72} = \sqrt{2}V_{D7}\cos\omega_S t, \\ i_{L71} &= \sqrt{2}I_{L71}\cos(\omega_S t - \phi_{L71}), \\ i_{L72} &= \sqrt{2}I_{L72}\cos(\omega_S t - \phi_{L72}). \quad \cdots\cdots (1) \end{aligned}$$

Let us assume that the source currents i_{D71} and i_{D72} on D7 are balanced with the power factor of $\cos\phi$, compensating the unbalanced components with reactive power control. The source-side currents i_{D71} and i_{D72} are expressed as

$$\begin{aligned} i_{D71} &= -i_{D72} \\ &= \sqrt{2}I_{D7}\cos(\omega_S t - \phi) \\ &= \sqrt{2}I_{D7p}(\cos\omega_S t + K\sin\omega_S t), \quad \cdots\cdots (2) \end{aligned}$$

where $\cos\phi = I_{D7p}/I_{D7}$. From (1) and (2), the output currents i_{PV71}, i_{PV72}, and i_{PV73} are given by

$$\begin{aligned} i_{PV71} &= i_{L71} - i_{D71}, \\ i_{PV72} &= -i_{L72} + i_{D72}, \\ i_{PV73} &= -i_{PV71} - i_{PV72}, \quad \cdots\cdots (3) \end{aligned}$$

Equation (3) gives the output currents of the HSPS to achieve the balanced source-side currents i_{D71} and i_{D72} on D7. The instantaneous power p_{PCS} flowing into the PCS of the HSPS, which consists of the three-leg PWM inverter, is given by

$$\begin{aligned} p_{PCS} &= v_{D71} \cdot i_{PV71} + v_{D72} \cdot i_{PV72} \\ &= (I_{L71}\cos\phi_{L71} + I_{L72}\cos\phi_{L72} - 2I_{D7}\cos\phi) \cdot V_{D7} \\ &\quad +(I_{L71}\cos\phi_{L71} + I_{L72}\cos\phi_{L72} \\ &\quad -2I_{D7}\cos\phi) \cdot V_{D7}\cos 2\omega_S t \\ &\quad +(I_{L71}\sin\phi_{L71} + I_{L72}\sin\phi_{L72} \\ &\quad -2I_{D7}\sin\phi) \cdot V_{D7}\sin 2\omega_S t. \quad \cdots\cdots (4) \end{aligned}$$

If the dc-capacitor voltage v_{DC7} is held constant by the constant dc-capacitor voltage control in the HSPS, the mean value $\overline{p}_{PCS}$ of the instantaneous p_{PCS} of (4) should be P_{PV} because the power P_{PV} generated by PV flows into the dc capacitor C_{DC} in Fig. 4, where P_{PV} is given by

$$P_{PV} = v_{DC7} \cdot I_{PV}. \quad \cdots\cdots (5)$$

This means that the constant dc-capacitor voltage control can calculate the active current I_{D7p} of the load currents i_{L71} and i_{L72}. From (4) and (5), thus, I_{D7p} is given by

$$\begin{aligned} I_{D7p} &= I_{D7}\cos\phi \\ &= \frac{I_{L71}\cos\phi_{L71} + I_{L72}\cos\phi_{L72}}{2} - \frac{P_{PV}}{2V_{D7}}. \quad \cdots\cdots (6) \end{aligned}$$

Equation (6) shows that the constant dc-capacitor voltage control can calculate the active current I_{D7p} in (2), where I_{D7p} is the theoretical RMS value of the source-side balanced active current with the unbalanced load currents i_{L71} and i_{L72} on D7 [21]. Thus, maintaining the dc-capacitor voltage v_{DC7} to a constant voltage by the constant dc-capacitor voltage control achieves the balanced source-side currents i_{D71} and i_{D72} with a power factor of $\cos\phi$. According to the regulations [22], a power factor of 0.9 is acceptable for home appliances in Japan. K in (2) is given by

$$K = \tan(\cos^{-1} 0.9). \qquad (7)$$

The proposed control strategy can improve power quality on the source side suppressing the voltage-rise-phenomena at Node3. Improving the source-side power quality, is to balance the secondary-side currents of the PMDT, reduces the losses in the PMDTs. Thus, the created-additional loss in feeders caused by a larger current flow with the reactive power consumption can be mitigated.

The dc-capacitor voltage v_{DC7} of the single-phase PWM inverters is detected, and then the difference Δv_{DC7} between the reference value V^*_{DC7} and the detected v_{DC7} is amplified by the PI controller. Here, (4) shows that the $2\omega_S$ component exits in addition to the dc component. Thus the detected v_{DC7} includes the $2\omega_S$ with the dc component. The $2\omega_S$ component in I_{D7p} causes third-order harmonics for i^*_{D7}. This affect the total harmonic distortion (THD) values of the source-side currents i_{D71}, i_{D72}, i_{D81}, i_{D82}, i_{D91}, and i_{D92}. Thus, a moving-average low-pass filter (MALPF) is used to remove this $2\omega_S$ component. The output value of the PI controller is inputted into the MALPF. After filtering with the MALPF, the effective value I_{D7p} of the source-side currents i_{D71} and i_{D72} at the PCC is obtained by performing constant dc-capacitor voltage control. The reference active component i^*_{D7p} is calculated by multiplying I_{D7p} by $\sqrt{2}\cos\omega_S t$. The reference reactive component i^*_{D7q} is also calculated by multiplying by I_{D7p} by $\sqrt{2}\sin\omega_S t$ and the gain K. According to the regulations [22], a power factor of 0.9 at the PCCs on low-voltage distribution feeders is acceptable. Thus, the control gain $K = \tan(\cos^{-1} 0.9)$ is used in this paper. The reference source current i^*_{D7} is given by

$$\begin{aligned} i^*_{D7} &= i^*_{D7p} + i^*_{D7q} \\ &= \sqrt{2}I_{D7p}(\cos\omega_S t + K\sin\omega_S t). \qquad (8) \end{aligned}$$

To detect the electrical angle $\theta_S = \omega_S t$ of the voltage v_{73} at the PCC a single-phase PLL algorithm is used [34]. The detected v_{73} corresponds to the α-phase component v_α, and the delayed voltage through the $T_S/4$ delay block corresponds to the β-phase component v_β. Using $\cos\theta_S$ and $\sin\theta_S$, v_α and v_β are transformed to v_d and v_q, respectively, in d-q coordinates. When the q-phase component v_q is equal to zero, it is possible to generate an electrical reference angle θ_S that is synchronized with v_{73}, which has an angular frequency of ω_S. Finally, the reference currents for the HSPS are calculated as

$$\begin{aligned} i^*_{71} &= i_{L71} - i^*_{D7}, \\ i^*_{72} &= -i_{L72} + i^*_{D7}, \\ i^*_{73} &= -i^*_{71} - i^*_{72}. \qquad (9) \end{aligned}$$

It is well known that a steady-state error remains when current feedback control based on the sine-triangle intercept technique with a PI controller is used in a single-phase PWM inverter. PI controllers in dq coordinates are used to control the output currents i_{71}, i_{72} and i_{73} of the HSPS. In Fig. 4, the reference value i^*_{71} is delayed by $T_S/4$, where T_S is the cycle of the voltage v_{73} at the PCC. i^*_{71} corresponds to the α-component, and the delayed current through the $T_S/4$ delay block corresponds to the β-components. Using θ_S, the electrical angle of the v_{73} generated by the PLL, the α- and β- components are transformed into i^*_{d1} and i^*_{q1}, respectively. The output current i_{71} is also transformed into i_{d1} and i_{q1} in the same way. The differences between the reference currents i^*_{d1} and i^*_{q1} are amplified by the PI controller in dq coordinates. The amplified values are retransformed into the α-component. Using the PWM technique, the gate signals for the power switching devices of the HSPS are then generated.

3. Simulation Results

A digital computer simulation was implemented to confirm the validity and practicability of the proposed voltage-rise-suppression and source-side current balancing with the constant dc-capacitor voltage-control-based reactive power control strategy for the HSPS using PSIM software. Table 2 shows the circuit constants, that were used in the computer simulation. $K_P = 0.7$ and $T_I = 20$ ms were used in the PI controller for constant dc-capacitor voltage control, and $K_P = 0.04$ and $T_I = 8$ ms were used in the PI controllers for current feedback control in d-q coordinates in Fig. 4 in the following simulation results.

Figure 5 shows simulation results for Fig. 2, where the reactive power control algorithm is not included in the control circuit of the HSPSs. v_{S1} and v_{S2} are the secondary-side source voltages of the PMDT. i_{S1} and i_{S2} are the secondary-side source currents of the PMDT. v_{D71} and v_{D72} are the receiving-end voltages at the PCC. i_{D71} and i_{D72} are the source-side currents on Service-wire7. i_{L71} and i_{L72} are the

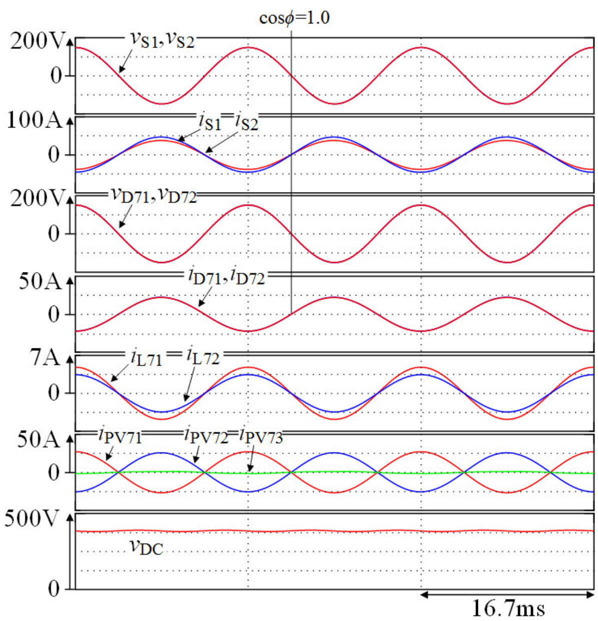

Fig. 5. Simulation waveforms for Fig. 2 without reactive power control

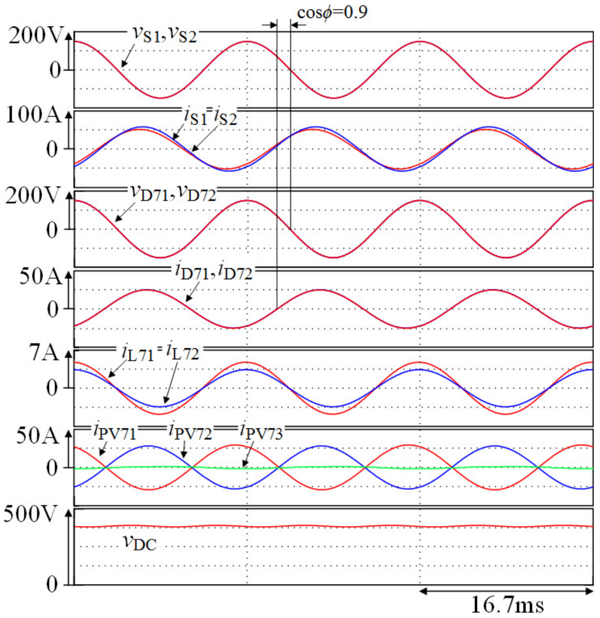

Fig. 6. Simulation waveforms for Fig. 2 with the proposed voltage-rise-suppression

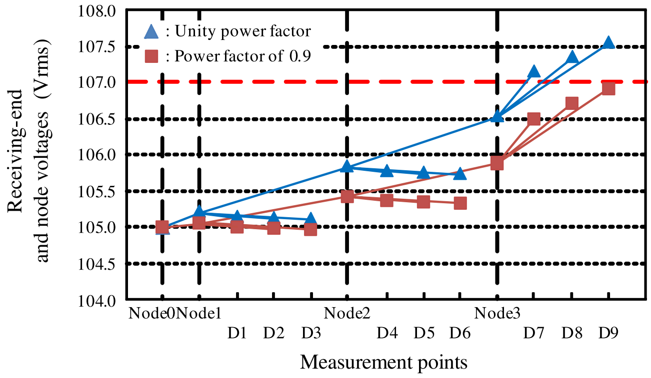

Fig. 7. RMS values of receiving-end voltages for each domestic consumer

load currents of Home7. i_{PV71}, i_{PV72}, and i_{PV73} are the output currents from the HSPS at Home 7. v_{DC7} is the dc-capacitor voltage. In the simulation results of Fig. 5, i_{S1}, i_{S2}, i_{L71}, and i_{L72} are unbalanced. However, the source-side currents i_{D71} and i_{D72} are balanced. i_{D71} and i_{D72} are in antiphase to the receiving-end voltages v_{D71} and v_{D72}. These generated power injections by the HSPS with these antiphase currents at Node3 cause the voltage rise at the PCC. The RMS values of v_{D71} and v_{D72} are 107.0 Vrms and 107.1 Vrms. Thus, the HSPS causes the voltage-rise phenomena at Node3.

Figure 6 shows simulation results for Fig. 2 with the proposed voltage rise suppression method and source-side current balancing. In the simulation results of Fig. 6, i_{S1}, i_{S2}, i_{L71}, and i_{L72} are unbalanced. However, the source-side currents i_{D71} and i_{D72} are balanced with a power factor of 0.9 with the proposed reactive power control. The THD values of i_{D71} and i_{D72} are 1.38% and 0.901%, respectively. These values satisfy the regulation [35]. The RMS values of v_{D71} and v_{D72} are 106.3 Vrms and 106.5 Vrms, respectively. Thus, the proposed voltage-rise-suppression method can suppress the voltage-rise phenomena at the PCC, improving the source-side currents quality.

Figure 7 shows simulated RMS values of the receiving-end voltages for each domestic consumer. The triangles show the RMS voltage for each domestic consumer without the proposed voltage-rise-suppression method. The maximum RMS value of the receiving-end voltage for each domestic consumer should be less than 107 Vrms according to the regulations in (19). However, without the reactive power control, the receiving-end voltages on D7, D8, and D9 exceed the maximum RMS value of 107 Vrms. As described before, power companies have to restrict the output power of HSPS on D7, D8, and D9. This restriction occurs in midday with fine weather. This is a serious problem for HSPSs because the profit from the sale of power decreases. The tetragons show the RMS voltage values for each domestic consumer with the proposed voltage-rise-suppression method, which is the constant dc-capacitor voltage-control-based reactive power control. The RMS values of the receiving-end voltages at all domestic consumers on D7, D8, and D9 are less than 107 Vrms, where the power factor on the source side on D7, D8, and D9 is controlled to 0.9. This power factor of 0.9 conforms to the regulations [22]. Thus, power companies can accept the power generated by the HSPS on D7, D8, and D9. The capacity of the PCS in the HSPS with the proposed reactive power control is larger by 8% as compared to that of the PCS in the HSPS with the unity power factor. Note that the PCS with the increased rating of only 8% can avoid the restriction of the output power of the HSPSs. This greatly improves the profit from the sale of power for domestic consumers. Improving the source-side currents quality can reduce the losses in the PMDT. Thus, the created-additional loss in feeders caused by a larger current flow with the reactive power consumption can be mitigated.

It is difficult to construct an experimental model for Fig. 2 in the laboratory. Thus, experimental validation with a reduced-scale experimental model for Fig. 2 is an important issue for further study.

4. Conclusion

This paper has proposed a voltage-rise-suppression and source-side current balancing strategy for the HSPSs connected to the PCC in SPTWDFs with the previously proposed constant dc-capacitor voltage-control-based reactive power control algorithm. The proposed reactive power control and load current balancing method uses only a constant dc-capacitor voltage control, which is always used in grid-connected inverters. No calculation blocks of the reactive and unbalanced active components of the load currents are necessary. Thus, the authors have provided the simplest algorithm to suppress the voltage rise at the PCC with balanced source-side currents. The basic principle of the constant dc-capacitor voltage-control-based strategy has been discussed in detail. The instantaneous power flowing into the PCS of HSPS has shown that the pre-defined power factor of 0.9, a value that conforms to Japanese regulations, is achieved with balanced source currents for domestic consumers connected to SPTWDFs with the constant dc-capacitor voltage-control-based strategy, suppressing the voltage rise at the PCC. A digital computer simulation has been implemented to confirm the validity and high practicability of the proposed control algorithm for HSPSs using a typical SPTWDF model in Japan. Simulation results have demonstrated that controlling the power factor to 0.9 on the source side by the HSPS with the proposed control method suppresses the voltage rise at the PCC, improving the source-side currents quality. The capacity of the PCS in HSPS with the reactive power control is larger by 8% as compared to that of the PCS with the unity power factor. Note that the PCS in HSPSs with the increased rating of only 8% can avoid the restriction on the output power of HSPSs. Thus, the authors have concluded that the proposed voltage-rise-suppression with the constant dc-capacitor voltage control is useful for practical HSPSs.

Finally, this paper is an improved and revised version of the conference paper (36). The authors would like to express their gratitude to the audience for their valuable discussions at the 18th ICEMS.

References

(1) [Online] Available: http://www.japaneselawtranslation.go.jp/law/detail_download/?ff = 09& id = 2573

(2) Japan Electric Association: "Grid-interconnection Code JEAC 9701-2012", pp.29–31 (2012) (in Japanese)

(3) R. Tonkoski, L.A.C. Lopes, and T.H. El-Fouly: "Coordinated active power curtailment of grid connected PV inverters for overvoltage prevention", *IEEE Trans. Sustain. Energy*, Vol.2, No.2, pp.139–147 (2011)

(4) Y. Ueda, K. Kurokawa, T. Tanabe, K. Kitamura, and H. Sugihara: "Analysis results of output power loss due to the grid voltage rise in grid-connected photovoltaic power generation systems", *IEEE Trans. Ind. Electron.,* Vol.55, No.7, pp.2744–2751 (2008)

(5) G.G. Pillai, G.A. Putrus, and N.M. Pearsall: "Impact of distribution network voltage-rise on PV system energy yield", in Proc. 12th Annu. IEEE Ind. Conf. (INDICON), 2013, Mumbai (2013)

(6) M.J.E. Alam, K.M. Muttaqi, and D. Sutanto: "A multi-mode control strategy for VAr support by solar PV inverters in distribution networks", *IEEE Trans. Power Syst.*, Vol.30, No.3, pp.1316–1326 (2015)

(7) P. Jahangiri and D.C. Aliprantis: "Distributed Volt/VAr control by PV inverters", *IEEE Trans. Power Syst.*, Vol.28, No.3, pp.3429–3430 (2013)

(8) E. Demirok, P. González, K.H.B. Frederiksen, D. Sera, P. Rodriguez, and R. Teodorescu: "Local reactive power control methods for overvoltage prevention of distributed solar inverters in low-voltage grids", *IEEE J. Photvoltaics,* Vol.1, No.2, pp.174–182 (2011)

(9) Y. liu, J. Bebic, B. Kroposki, J. de Bedout, and W. Ren: "Distribution system voltage performance analysis for high-penetration PV", in Proc. IEEE Energy 2030 Conf., 2013, Mumbai (2013)

(10) X. Liu, A. Aichhorn, L. Liu, and H. Li: "Coordinated control of distributed energy storage system with tap changer transformers for voltage rise mitigation under high photovoltaic penetration", *IEEE Trans. Smart Grid*, Vol.3, No.2, pp.897–906 (2012)

(11) M.J.E. Alam, K.M. Muttaqi, and D. Sutanto: "Distributed energy storage for mitigation of voltage-rise impact caused by rooftop solar PV", in Proc. IEEE PES General Meeting, pp.1–8, San Diego, California, USA. (2012)

(12) M.J.E. Alam, K.M. Muttaqi, and D. Sutanto: "Mitigation of rooftop solar PV impacts and evening peak support by managing available capacity of distributed energy storage systems", *IEEE Trans. Power Syst.*, Vol.28, No.4, pp.3874–3884 (2013)

(13) M.N. Kabir, Y. Mishra, G. Ledwich, Z.Y. Dong, and K.P. Womg: "Coordinated control of grid-connected photovoltaic reactive power and battery energy storage systems to improve the voltage profile of a residential distribution feeder", *IEEE Trans. Ind. Informatics*, Vol.10, No.2, pp.967–977 (2014)

(14) F. Marra, G.Y. Yang, Y.T. Fawzy, C. Traeholt, E. Larsen, R. Garcia-Valle, and M.M. Jesen: "Improvement of local voltage in feeders with photovoltaic using electric vehicles", *IEEE Trans. Power Syst.*, Vol.28, No.3, pp.3515–3516 (2013)

(15) Y. Mitani: "Method and System for Leveling Power Load", Japan Patent Office, 4862 153 (P4 862 153) (2012)

(16) [Online] Available: http://www.nissan-global/com/JP/NEWS/

(17) M. Yilmaz and P.T. Krein: "Review of benefits and challenges of vehicle-to-grid technology", in Proc. IEEE Energy Conversion Congress and Exposition (ECCE), pp.3082–3089 (2012)

(18) I. Cvetkovic, T. Thacker, D. Dong, G. Francis, V. Podosinov, D. Boroyevich, F. Wang, R. Burgos, G. Skutt, and J. Lesko: "Future home uninterruptible renewable energy system with vehicle-to-grid technology", in Proc. ECCE, pp.2675–2681 (2009)

(19) S. Takeno: "Electrical codes and facilities management", p.21, Tokyo Denki University Press (2015) (in Japanese)

(20) E.E. Pompodakis, L.A. Drougakis, L.S. Lelis, and M.C. Alexiadis: "Photovoltaic systems in low-voltage networks and overvoltage correction with reactive power control", *IET Renewable Power Correction*, Vol.10, No.3, pp.410–417 (2016)

(21) H. Tanaka, F. Ikeda, T. Tanaka, H. Yamada, and M. Okamoto: "Novel reactive power control strategy based on constant dc-capacitor voltage control for reducing the capacity of smart charger for electric vehicles on single-phase three-wire distribution feeders", *IEEE J. Emerg. Sel. Topics Power Electron.*, Vol.4, No.2 (2016)

(22) The Chugoku Electric Power Co., Inc.: "Electric-Supply Stipulation", p.46 (2012) (in Japanese)

(23) H. Sugihara: "A study on energy management in a residential area using low-voltage distribution network with high penetration of photovoltaic systems", presented at 31st Annu. Meeting Jpn. Society Energy and Resources, No.3-2 (2012) (in Japanese)

(24) [Online] Available: http://www.meti.go.jp/meti_lib/report/2013fy/E003416.pdf

(25) H. Akagi, Y. Kanazawa, and A. Nabe: "Instantaneous reactive power compensators comprising switching devices without energy storage components", *IEEE Trans. Ind. Appl.,* Vol.IA-20, No.3, pp.625–630 (1984)

(26) A. Nava-Segura and G. Mino-Aguilar: "Four-branches-inverter-based-active-filter for unbalanced 3-phase 4-wires electrical distribution systems", *Proc. IEEE Ind. Appl. Conf.,* Vol.4, pp.2503–2508 (2000)

(27) F.Z. Peng, G.W. Ott, and D.J. Adams: "Harmonic and reactive power compensation based on the generalized instantaneous reactive power theory for the three-phase four-wire systems", *IEEE Trans. on Power Electron.,* Vol.13, pp.1174–1181 (1998)

(28) B.N. Singh and P. Rast, "A new topology of active filter to correct power-factor, compensate harmonics, reactive power and unbalance of three-phase four-wire loads", *IEEE Appl. Power Electron. and Expo.,* Vol.1, pp.141–147 (2003)

(29) A. Adya, A.P. Mittal, and J.R.P. Gupta: "Modeling and control of DSTATCOM for three-phase, four-wire distribution systems", *IEEE-IAS Ann. Meeting,* Vol.4, pp.2428–2434 (2005)

(30) N. Geddada, S.B. Karanki, M.K. Mishra, and B.K. Kumar: "Modified four leg DSTATCOM topology for compensation of unbalanced and nonlinear loads in three phase four wire system", Proc. of EPE'11, pp.1–10 (2011)

(31) J.W. Dixon, J.J. Garcia, and L. Moran: "Control system for three-phase active power filter which simultaneously compensates power factor and unbalanced loads", *IEEE Trans. Ind. Electron.,* Vol.42, pp.636–641 (1995)

(32) A. Abllan, G. Garcera, M. Pascual, and E. Figueres: "A new current controller applied to four-branch inverter shunt active filters with UPF control method", Proc. of PESC'01, Vol.3, pp.1402–1407 (2001)

(33) H. Tanaka, T. Wakimoto, T. Tanaka, M. Okamoto, and E. Hiraki: "Reducing Capacity of Smart Charger for Electric Vehicles on Single-Phase Three-Wire Distribution Feeders with Reactive Power Control", *IEEJ Journal of IA*, Vol.3, No.6, pp.437–445 (2014)

(34) L.N. Arruda, S.M. Silva, and B.J.C. Filho: "PLL structures for utility connected systems", in Conf. Record of the 36th IEEE-IAS Annu. Meeting, pp.2655–2660 (2001)

(35) IEEE 519-2014: "Recommended Practices and Requirements for Harmonic Control in Electrical Power System", (2014)

(36) M. Ushiroda, T. Wakimoto, H. Yamada, T. Tanaka, M. Okamoto, and K. Kawahara: "Voltage rise suppression and load balancing by PV PCS with constant dc-capacitor voltage control based strategy on single-phase three-wire distribution feeders", in Proc. 18th Int. Conf. on Electrical Machines and Systems (ICEMS), 27C4-5 (2015)

Mitsumasa Ushiroda (Non-member) received the B.E. degree in electrical and electronic engineering from Yamaguchi University in 2015. He was engaged in research on a voltage-rise suppression and power quality control strategy for photovoltaic power conditioning system in SPTWDFs.

Takaaki Wakimoto (Non-member) received the B.E. degree in electrical and electronic engineering from Yamaguchi University in 2013. He was engaged in research on a voltage rise suppression and source-side current balancing strategy for photovoltaic power conditioning system on SPTWDFs with the constant dc-capacitor voltage-control-based reactive power control.

Hiroaki Yamada (Member) received the M.E. degree from Shimane University in 2004. In 2007, he received the Doctor of Engineering from Yamaguchi University (YU). From 2007 to 2010, he was a Lecturer at Kushiro National College of Technology. From 2010 to 2014, he was an Assistant Professor at Kyushu Institute of Technology. Since 2014, he has been a Lecturer in the Department of Electrical and Electronic Engineering at YU. His research interests are on drawback current compensation and LED power supply. Dr. Yamada is a member of the IEEE.

Toshihiko Tanaka (Fellow) was born in Hokkaido, Japan, in 1959. He received the M.E. degree from Nagaoka University of Technology in 1984. In 1995, he received the Ph.D. degree in Engineering from Okayama University. He joined Toyo Denki Mfg. Co. in 1984. From 1991 to 1997, he was an Assistant Professor at the Polytechnic University of Japan. From 1997 to 2004 he was an Associate Professor at Shimane University. Since 2004, he has been a Professor in the Department of Electrical and Electronic Engineering at Yamaguchi University. His research interests are on harmonics generated by static power converters and their compensation. Dr. Tanaka is a member of the IEEE.

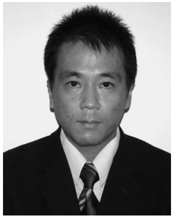

Masayuki Okamoto (Member) received the M.E. and Ph.D. degrees in electrical engineering from Yamaguchi University (YU) in 1996 and 1999, respectively. From 1999 to 2012, he was an Assistant Professor at YU. From 2012 to 2017, he was an Associate Professor at National Institute of Technology, Ube College. He is currently a Professor. His research interests include device modeling of GaN-based switching devices and design of high-frequency power electronic converters with the switching devices. Dr. Okamoto is a member of the IEEE.

Koji Kawahara (Senior Member) was born in Hiroshima, Japan, in 1965. He received M.E. and D.Eng. degrees from Hiroshima University in 1990 and 1999, respectively. He is a professor of the Department of Electrical Systems Engineering, Hiroshima Institute of Technology, Japan. He was an academic visitor of the University of Manchester Institute of Science and Technology, from 2003 to 2004. His research interests lie in power system operation and planning. Dr. Kawahara is a senior member of the IEEE.